

Highly Photocatalytic Activity of Novel CuFe₂O₄/GO Nano Composite in the Degradation of Phenol from Aqueous Solution

Giang H. Le¹, Quyet T. Ngo¹, Tuan T. Nguyen^{1,2}, Quang K. Nguyen¹, Trang T. T. Quan¹, Tuan A. Vu^{1,2,*}

¹Institute of Chemistry, Vietnam Academy of Science and Technology (VAST), 18 Hoang Quoc Viet, Cau Giay District, Hanoi, Vietnam

²Graduate University of Science and Technology, Vietnam Academy of Science and Technology, 18 Hoang Quoc Viet, Cau Giay District, Hanoi, Vietnam

Abstract The CuFe₂O₄/Graphene oxide (GO) composite was successfully synthesized by co-precipitation in “situ” using FeCl₃.6H₂O and CuCl₂.2H₂O as iron and copper sources on GO and followed by thermal reduction. The product was characterized by XRD, XPS, TEM, BET and FTIR. From the XRD and XPS results, it reveals the formation of copper ferrites spinel CuFe₂O₄ on GO surface. From TEM images, it showed that CuFe₂O₄/GO composite has particle size of 20-30 nm and uniform size distribution. The as-prepared CuFe₂O₄/GO nano composite was used to test the photocatalytic degradation of phenol from aqueous solution. After 90 minutes of reaction, the conversion (calculated according COD) reached to the value of 90%, indicating highly photocatalytic activity of this catalyst. Moreover, after three recycles, the photocatalytic activity was almost unchanged as compared to that of fresh catalyst, indicating the relatively high stability and it can be reused. Additionally, this CuFe₂O₄/GO composite showed highly magnetic property so it can be easily recovered by applying the magnetic field out side.

Keywords Nanocomposite CuFe₂O₄/GO, Simulated sun-light irradiation, Photocatalytic phenol degradation

1. Introduction

In recent years, graphene based materials (graphene and graphene oxide) have received a special attention due to its unique structure and physical chemical properties as well as their utilization in a variety of applications such as electrode in batteries and super capacitors, conductive matrix, support material and adsorbents in environment [1]. Graphene, a two-dimensional nano material with several layers of sp² hybridized carbon atoms arranging in six-membered rings, has showed unique properties including, high Young's modulus (ca. 1100 GPa), high strength (125 GPa), high thermal (5000 W.m⁻¹.K⁻¹) and electrical (0,96 x 10⁻⁶ W⁻¹.m⁻¹) conductivities at room temperature, high specific surface area (theoretical value 2630 m².g⁻¹) and high chemical stability [1, 2a-c]. Due to its can be used excellent electric conductivity and high surface area, graphene based materials as suitable material used as two-dimensional platform to accept and spread photogenerated electron-hole pairs from semiconductor upon light irradiation, enhancing the photodegradation efficiency of semiconductor in

photodegradation reaction [3, 4]. The spinel structured ferrites have the general formula MFe₂O₄ (M: Fe, Co, Ni, Zn, Cu, etc.). The properties of the ferrite can be varied by changing the identity of the divalent M²⁺ cation. Among the ferrites, copper ferrite nanoparticles (CuFe₂O₄) has received a great interest and is widely used in electronics, and catalysis [5, 6, 7]. CuFe₂O₄ is one of the iron-based cubic spinel series showing advantages of a narrow band gap (1.9eV) for high absorption efficiency of sunlight, high photochemical stability, and excellent ferromagnetic properties for catalyst recovery by applying magnetic field [7]. However, CuFe₂O₄ nanomaterial used as a photocatalyst in the degradation of pollutants is still already investigated. However, the CuFe₂O₄ nanoparticles are tended to aggregate due to the ferromagnetic properties, forming large particles. Moreover, because of the narrow band-gap resulted in the rapid recombination of electrons and hole it caused the fast decreased of their photo catalytic activity.

To overcome this recent years, different magnetic iron oxides graphene nano composites, have been synthesized and it claimed that the dispersion and attachment of metal oxide particles can be improved, resulting in enhance of photocatalytic performance in the degradation of organic compounds as compared with metal oxide itself or pristine graphene [3, 8, 9]. The improvement of photocatalytic

* Corresponding author:

vuanhtuan.vast@gmail.com (Tuan A. Vu)

Published online at <http://journal.sapub.org/pc>

Copyright © 2017 Scientific & Academic Publishing. All Rights Reserved

performance can be explained due to the special ability of graphene, GO which can act as electron acceptor/shuttle photogenerated from metal oxide upon light irradiation. This makes life span of photoexcited electron-hole pairs longer, thereby hindering the electron-hole recombination and enhancing photoactivity of materials. Additionally, graphene oxide has abundant oxygenated functional groups such as hydroxyl, epoxides and carboxyl groups, easily formed the covalent bond with metal ions and can be more suitable to disperse CuFe_2O_4 nano particles on GO surface.

In this paper, we report a two-step synthesis of $\text{CuFe}_2\text{O}_4/\text{GO}$ composites through co-precipitation in "situ" and thermal reduction and photo-fenton activity in the degradation of Phenol. Effects of pH, catalyst dosage as well as stability of the catalysts investigated.

2. Experimental

2.1. Synthesis of GO

Graphene oxide is synthesized by chemical oxidation and exfoliation of natural graphite using modified Hummers method [10]. GO powders were exfoliated by the treatment in a microwave oven (Model MWO-G20SA) in ambient conditions at 700 W for one minute [11]. Upon microwave irradiation, the volume expansion of the GO powders much is larger than the exfoliated by using the common method (ultrasonic treatment)

2.2. Synthesis of $\text{Fe}_3\text{O}_4/\text{GO}$ Nano Composite

Magnetic iron oxide - graphene oxide composites ($\text{Fe}_3\text{O}_4/\text{GO}$) were prepared by co-precipitation using $\text{FeCl}_3 \cdot 6\text{H}_2\text{O}$ and $\text{FeCl}_2 \cdot 4\text{H}_2\text{O}$ as iron-containing sources and deposited on GO surface. Suspension of GO was diluted with distilled water under vigorous stirring. After that, the mixture of FeCl_3 and FeCl_2 (ratio $\text{Fe}^{3+}/\text{Fe}^{2+}:2/1$) was slowly added to the GO mixture. The mixture was adjusted solution pH value by adding 15 mL NH_4OH 30% to reach the pH value of 10. The obtained gels were maintained at 80 °C for 45 minute. The product was repeatedly washed by distillation water and ethanol until pH value of 7. The final product was dried in vacuum oven at 60 °C before use. The ratio of magnetite to GO (in weight) is 1:3.

2.3. Synthesis of $\text{CuFe}_2\text{O}_4/\text{GO}$ Nano Composite

Nanocomposite $\text{CuFe}_2\text{O}_4/\text{GO}$ was synthesized by co-precipitation in "situ" using $\text{FeCl}_3 \cdot 6\text{H}_2\text{O}$ and $\text{CuCl}_2 \cdot 2\text{H}_2\text{O}$ as iron and copper sources on GO and followed by the thermal reduction. Firstly, 225 mg GO was added into 110 mL of distilled water, ethanol solution mixture was treated in a ultrasonic bath for 30 minute. After that, 53.5 mg of $\text{CuCl}_2 \cdot 2\text{H}_2\text{O}$ and 169.1 mg of $\text{FeCl}_3 \cdot 6\text{H}_2\text{O}$ were added to 110 mL of distilled water and ethanol under stirring condition for 15 min. at room temperature. The above two mixtures were put together and stirred for 30 min. After that, the mixture was adjusted to

pH value of 10 by adding 15 mL NH_4OH 30% solution and stirred for 3 h. The obtained products were repeatedly washed by distillation water until pH of 7 and then freeze dried. Finally, the obtained product was calcined by heating at 650 °C for 2 h in nitrogen atmosphere. The ratio of $\text{CuFe}_2\text{O}_4/\text{GO}$ (in weight %) is 1:3.

2.4. Characterization

The powder X-ray diffraction (XRD) patterns of the samples were recorded on a Shimadzu XRD-6100 analyzer with Cu K α radiation (1.5417 Å). Transmission electron microscopy (TEM) using JEOL 1010 instrument operating at 80 kV with magnification of 25,000–100,000. The X-ray photoelectron spectroscopy (XPS) measurement was performed on the ESCALab MKII spectrometer using Mg K α radiation. A vibrating-sample magnetometer (VSM, PPMS6000, Quantum Design) was used to study the magnetic properties of magnetite nano particles. The FT-IR spectra of the samples were measured by the KBr pellet method (BIO-RAD FTS-3000). Surface Area of samples was determined on Quantachrome Instruments version 3.0 at 77 K and using nitrogen adsorbed. Energy-dispersive X-ray spectroscopy (EDX) of samples were measured using JEOL JED-2300 spectrometer.

2.5. Photo-Fenton Reaction

Pyrex glass bottles, in which a 100 mL aliquot of each phenol solution with initial concentrations of 100 mg/L was added. Photocatalytic degradation of phenol from aqueous solution was carried out in a batch reactor at the following conditions: photocatalyst conc. of 0.05 - 0.1 g/L and H_2O_2 conc. of 136 mg/L. Photo-Fenton reaction of phenol was performed under stirring condition, at room temperature and pH in the range of 2.5 – 8.0. The pH value of reactant solution was adjusted with HCl 0.01 M or NaOH 0.01 M solution. The samples were collected at different reaction time. Simulated sunlight source was used UV-A range lamps (4 lamps, power of 15W for each lamp). The emission spectrum between 400 and 800 nm follows the solar spectrum. Before starting the illumination, each reaction mixture was stirred for 25 minute in the dark in order to reach the adsorption-desorption equilibrium between the phenol and the catalysts. Concentrations of phenol and the intermediates formed the processes were determined by using high performance liquid chromatography (HPLC – Agilent 1100) with detector DAD (Agilent - US). The assessment of the photodegradation was also examined by chemical oxygen demand (COD). The COD was measured by potassium dichromate titrimetric method by using Lambda 35 UV-vis spectrophotometer intensities of the band at 610 nm.

The COD removal efficiency (H %) was calculated as following equation:

$$\text{COD removal efficiency (H\%)} = \frac{\text{COD}_o - \text{COD}_t}{\text{COD}_o} \times 100$$

Where COD₀ is the COD initial of phenol and COD_t is the COD after the different time.

3. Results and Discussion

3.1. X-ray Diffraction (XRD) and Fourier Transform Infrared Spectroscopy (FTIR) Analysis

The X-ray diffraction pattern of the CuFe₂O₄/GO composite was shown in Fig. 1a. The diffraction peaks (30.1 °, 35.4 °, 43.3 °, 57.2 °, 62.7 °) of CuFe₂O₄/GO corresponded to the (220), (311), (400), (511), (440) planar of face-centered cubic structure of CuFe₂O₄ as reported in the literature [8, 12]. The absence of the peak at 2θ of 11 ° (fig. 1b) which is characteristic for GO structure, indicated the intercalation of CuFe₂O₄ nanoparticles within GO layers. Additionally, nano CuFe₂O₄ particles generated on the GO surface prevent the restacking of GO sheets to form regular and periodic layered structure of graphite [13]. However, no typical peak of graphene at 2θ of 23-26,3 ° was observed, suggesting that the graphene sheets were exfoliated [14].

The FTIR spectrum of CuFe₂O₄/GO was presented in Fig. 1c. The band at 3419 cm⁻¹ is attributed to the stretching vibration of O–H. Strong bands in the region of 1620 – 1235

cm⁻¹ correspond to the C=C stretching vibration, the C–O–H deformation vibration, respectively. The band with low intensity at 2342 cm⁻¹ assigned to CO₂ – GO bending vibrations [15]. The new bands at 530 cm⁻¹ and 437 cm⁻¹, appeared indicating the interaction between CuFe₂O₄ and the graphene oxide sheets through metal-carbonyl coordination [8].

3.2. Transmission Electron Microscopy (TEM) and Energy-dispersive X-ray Spectroscopy (EDX) Analyses

The image of CuFe₂O₄ was shown in Fig. 2a. As observed in Fig. 2a CuFe₂O₄ nanoparticles anchored on GO sheets and relatively well distributed. It could be noted in Fig. 2a that the size of the CuFe₂O₄ on GO was around 20–30 nm with a relatively narrow size distribution and a certain extent of particles aggregation. The elemental composition of the hybrid was examined by EDX spectroscopy and the results were present in Fig. 2b. From analysis result, it shows that CuFe₂O₄/GO contained 43.79% C in weight, 27.51% O in weight, 22.87% Fe in weight and 5.84% Cu in weight, while the Fe₃O₄/GO contained 40.89% C in weight, 34.75% O in weight and 24.20% Fe in weight, respectively. This revealed that CuFe₂O₄ and Fe₃O₄ have the similar composition.

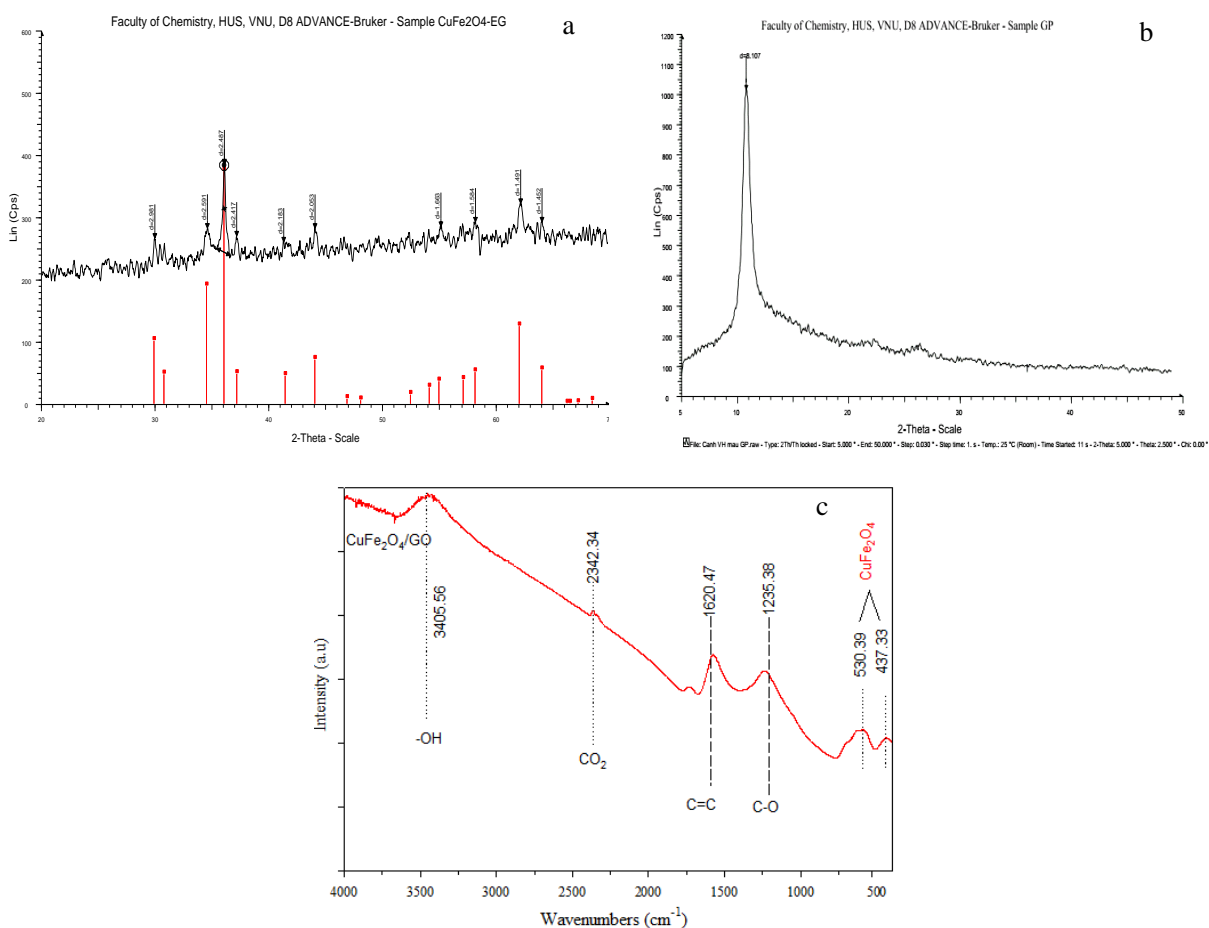


Figure 1. XRD patterns of CuFe₂O₄/GO (a); GO (b) and (c) FT-IR spectra of CuFe₂O₄/GO

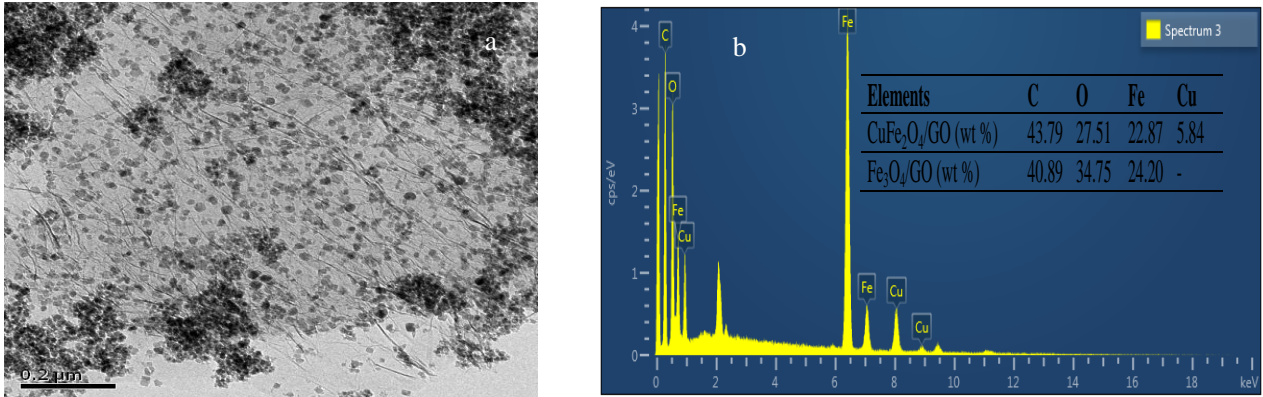


Figure 2. TEM images (a) and EDX spectra (b) of CuFe₂O₄/GO

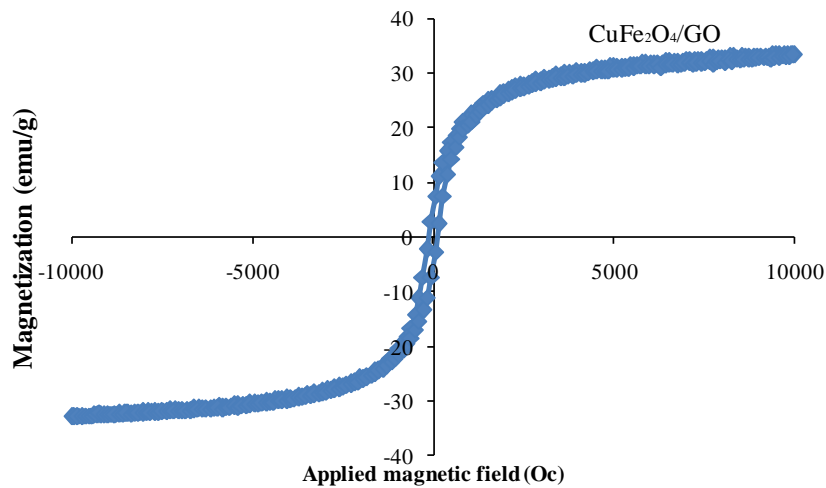


Figure 3. Magnetization curve of CuFe₂O₄/GO

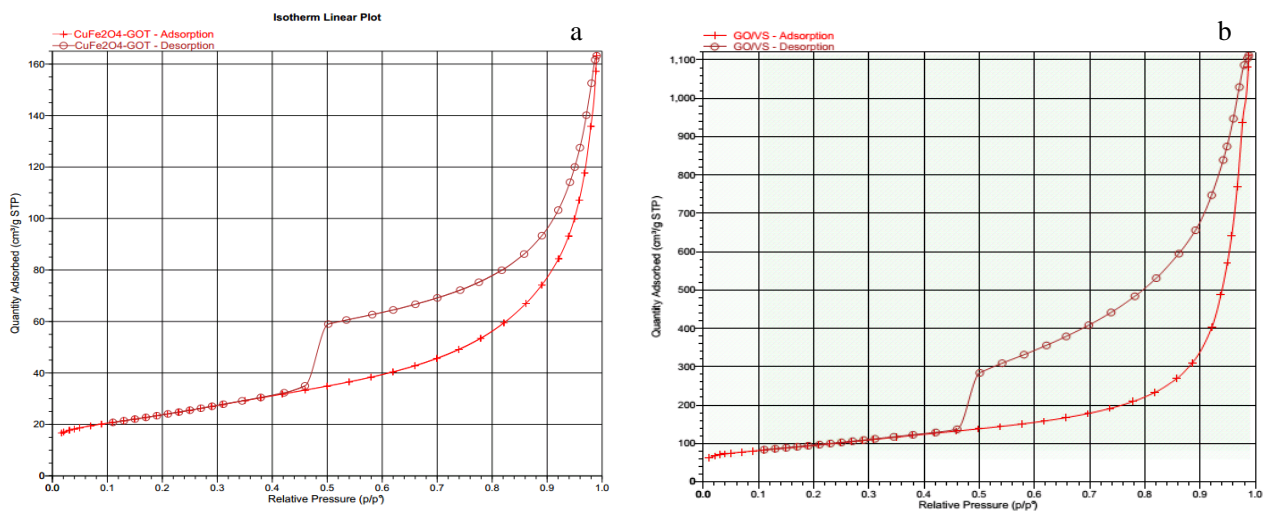


Figure 4. N₂ adsorption – desorption isotherms of CuFe₂O₄/GO (a) and GO (b)

3.3. Magnetization of CuFe₂O₄/GO

Fig. 3 shows the magnetization hysteresis loop of the the CuFe₂O₄/GO nanostructures. The magnetic hysteresis loops

were Slike curves. The results showed no remanence or coercivity in the hybrids suggesting that there was no remaining magnetization when external magnetic field was removed and the magnetic composites were

superparamagnetic. The saturated magnetization of the superparamagnetic was nearly 35 emu/g which guaranteed catalyst separation by applying magnetic field out side.

3.4. N₂ Adsorption–Desorption Isotherms (BET) Analysis

N₂ adsorption–desorption isotherms of CuFe₂O₄/GO composites and GO are shown in figure 4. The N₂ adsorption-desorption curve of CuFe₂O₄/GO composites displayed type IV with hysteresis corresponding to the capillary condensation which is typical for mesoporous material [16]. Thus, mesopore volume of composite reach 99% of total pore volume (0.524 cm³/g). This indicates that in the pore distribution, micropore volume is only minor. The pore texture parameters and surface area were listed in table 1. CuFe₂O₄/GO composites and GO had pore diameter of 8.8 to 21 nm and surface area of 183 m²/g and 331 m²/g, respectively. Note that GO has a main contribution of mesopore volume larger surface. CuFe₂O₄/GO particles were

well dispersed on GO surface and consequently particles size is smaller (i.e surface area of particles is higher) due to the suppressing particles aggregation. However, the deposition and intercalation of CuFe₂O₄ particles within GO layers caused the decrease of surface area and pore volume as compared to that of the pure GO.

Table 1. Textual characteristics of CuFe₂O₄/GO and GO

Samples	Specific surface area S _{BET} (m ² /g)	Micro-pore volume (cm ³ /g)	Total pores Volume (cm ³ /g)	Pore diameter (nm)
CuFe ₂ O ₄ /GO	183	0.0043	0.524	8.3-11.9
GO	331	0.0015	1.716	7.8-21.2

3.5. The X-ray Photoelectron Spectroscopy (XPS) Analysis

XPS spectra of CuFe₂O₄/GO were show in fig. 5.

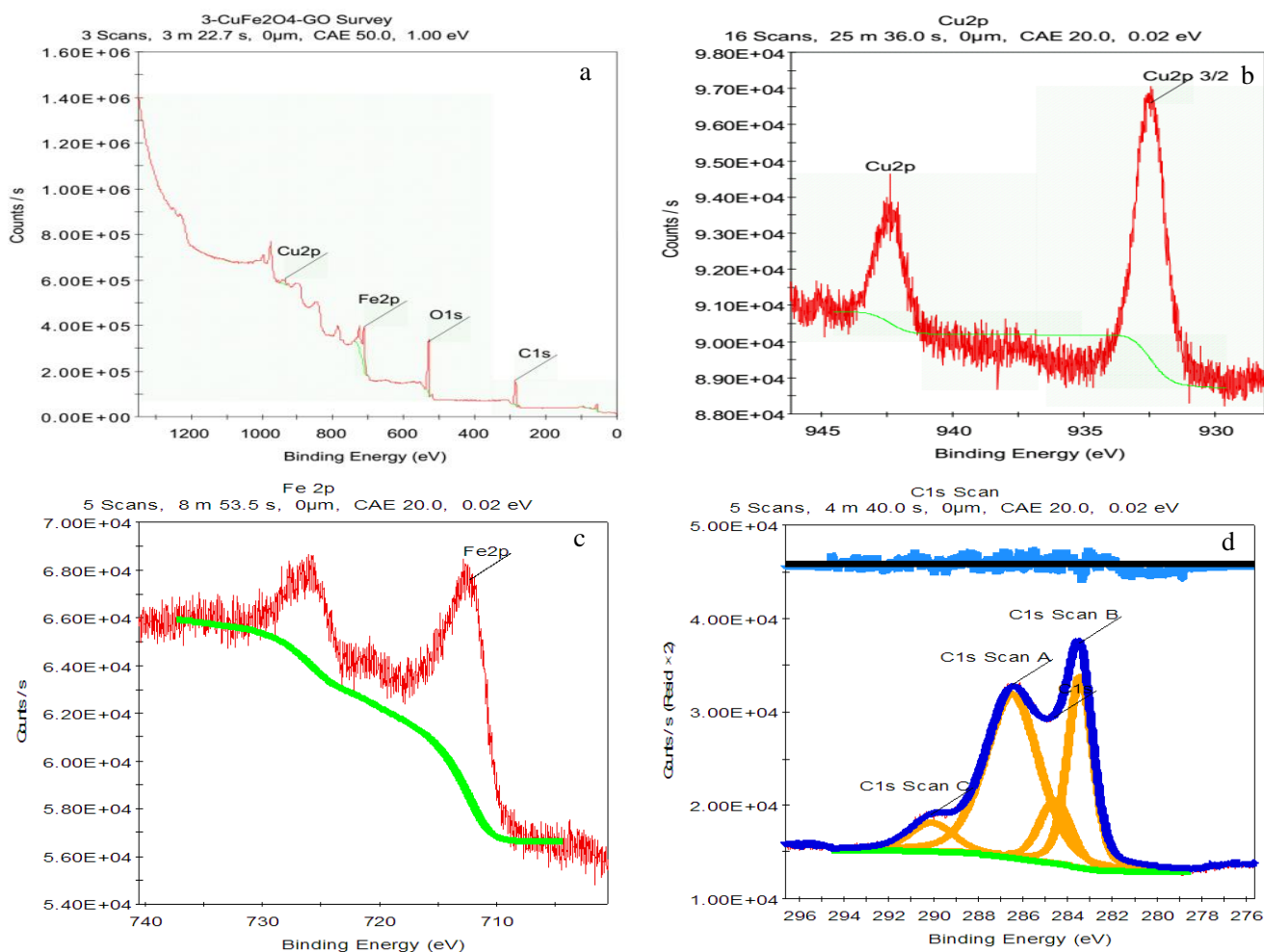


Figure 5. XPS spectra of CuFe₂O₄/GO

The widely scan of the $\text{CuFe}_2\text{O}_4/\text{GO}$ showed photoelectron lines at binding energy of 285 eV, 530 eV, and 711 eV correspond to the C1s, O1s, and Fe2p, respectively (Fig. 5). The deconvolution of the C1s peak was consisted of three peaks at 284.4 eV, 285.6 eV and 288.3 eV, which were ascribed to the C-C, C-O, and C(O)O in GO sheets. In the case of XPS spectra of C1s, the peak appeared at 291 eV was assigned to the $\pi-\pi^*$ bond of rGO, GO [17]. Additionally the peak at 291 eV is attributed to the bonding state between electron pairs and holes in GO and rGO structures [18]. The binding energy of $\text{Fe}2p_{3/2}$ of the hybrid was located at 711 eV while the peak of $\text{Fe}2p_{1/2}$ appeared at 725 eV. As observed in figure 5d, no peak at 932 eV and 941 eV which are characteristic for individual existence of Cu^+ and Cu^{2+} indicated that no copper oxides were separately formed. The high-resolution XPS spectra of Cu2p and Fe2p (Figure 5c,d) indicated that oxidation state of Cu and Fe being Cu^{2+} and Fe^{3+} , respectively in the CuFe_2O_4 nanocomposite [19].

3.6. Photocatalytic Activity

a/ Effect of catalyst dosage

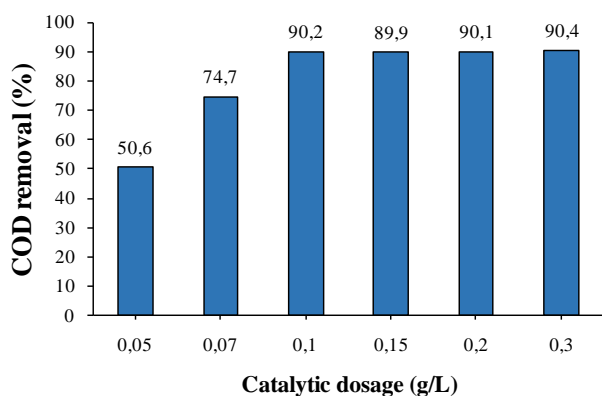


Figure 6. Effect of catalyst concentration on degradation of phenol, [Phenol] = 100 mg/L, $[\text{H}_2\text{O}_2]$ = 136 mg/L pH = 3; T = 303 K

The effect of different of catalyst concentrations on phenol degradation $\text{CuFe}_2\text{O}_4/\text{GO}$ is shown in Fig. 6. The removal efficiency increases from 50.6% to 90.4% with increasing of $\text{CuFe}_2\text{O}_4/\text{GO}$ concentration from 0.05 g/L to 0.3 g/L. However, no significant difference in removal of phenol by further increasing concentration of $\text{CuFe}_2\text{O}_4/\text{GO}$ from 0.1 to 0.3 g/L was observed. As expected, the amount of active sites on $\text{CuFe}_2\text{O}_4/\text{GO}$ rose with increasing dosage of catalyst, which promoted the generation of radicals, and the higher reaction rate is achieved. This can be explained that OH^\cdot radicals decomposed more rapidly, but the reaction occurred not rapid enough to consume the OH^\cdot radicals generated [9]. Therefore, the use of higher catalyst concentration of 0.1 g/L is not necessary.

b/ Effect of pH

As seen from Fig. 7, pH has an important influence on the degradation of phenol due to its role in controlling the

activity of the oxidant agents and the substrates, the domination of iron species, and the stability of hydrogen peroxide. The COD removal efficiency of phenol degradation over $\text{Fe}_3\text{O}_4/\text{GO}$ was almost 62% at pH value of 3, when pH of phenol solution increased to higher than 5, the COD removal efficiency was less than 20%. While, the initial pH value difference hardly affects on the degradations of Phenol on $\text{CuFe}_2\text{O}_4/\text{GO}$. The optimum pH was found to be 3, where the rate of the reaction is the fastest. This can be rationalized that pH increased above 5, the reaction rate decreased sharply possibly due to the formation of inactive ferryl ion FeO^{2+} (the lower oxidation potential of hydroxyl radicals), causing the deactivation of catalyst [8, 20].

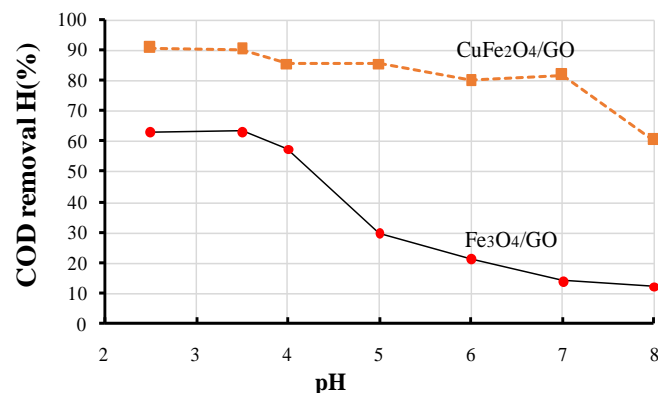


Figure 7. Influence of pH values on phenol degradation over $\text{Fe}_3\text{O}_4/\text{GO}$ and $\text{CuFe}_2\text{O}_4/\text{GO}$ composites

c/ Photo-Fenton degradation

In this study, the catalytic activities of two samples were tested under different reaction conditions are presented in Fig. 8. The experiments were carried out at: pH: 3, H_2O_2 concentration: 136 mg/L, catalyst dosage: 0.1 g/L, Phenol initial concentration: 100 mg/L.

From Figure 8a, it is observed that after 90 minutes of reaction under the simulated sunlight irradiation, the conversion (calculated according COD) reached 90% for $\text{CuFe}_2\text{O}_4/\text{GO}$ and 62% for catalyst $\text{Fe}_3\text{O}_4/\text{GO}$. To figure out the difference in photo-fenton and fenton activity, phenol degradation of $\text{CuFe}_2\text{O}_4/\text{GO}$ was investigated. Under the same reaction conditions but no light irradiation, the conversion reached to the value of 75%. Photocatalytic activity on phenol degradation over $\text{CuFe}_2\text{O}_4/\text{GO}$ higher than $\text{Fe}_3\text{O}_4/\text{GO}$ can be explained as follows: the iron oxide Fe_3O_4 with the band gap energy of 2.2 - 2.7 eV, GO substrate contributes to the electron transfer from the conduction band of the semiconductor, limited recombination electrons and holes. For CuFe_2O_4 , due to the electronics configuration changes the band gap energy of 1.5 - 2 eV is smaller than that of Fe_3O_4 increasing the ability to generate OH^\cdot radicals. Moreover, the presence of Cu ion in CuFe_2O_4 can reduce Fe^{3+} to Fe^{2+} ion which increased OH^\cdot radical generation, leading to increase the photo-fenton reaction rate [21, 22].

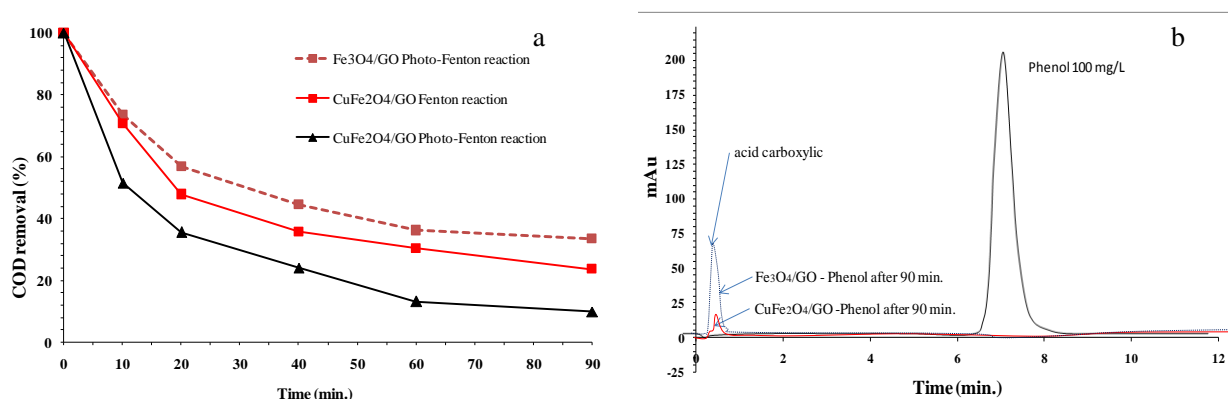


Figure 8. (a) Comparison of the photocatalytic degradation of phenol solution under different conditions. (b) HPLC diagram of phenol degradation over $\text{CuFe}_2\text{O}_4/\text{GO}$

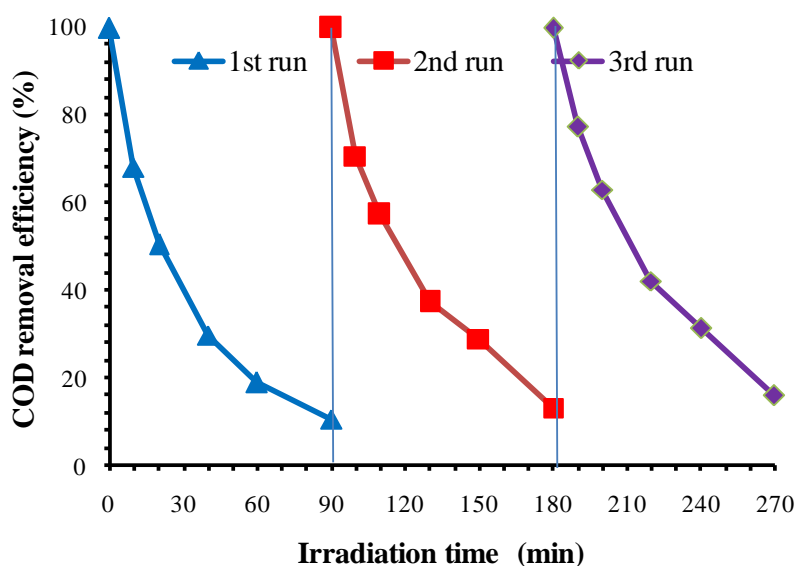


Figure 9. The cycling runs of phenol degradation over $\text{CuFe}_2\text{O}_4/\text{GO}$ composite under simulated solar irradiation, experimental conditions: [Phenol] = 100 mg/L, $[\text{H}_2\text{O}_2]$ = 136 mg/L, catalyst dosage = 0.1 g/L, pH = 3, T = 303K

Figure 8b showed that after 90 minutes, almost phenol was converted to CO_2 and H_2O . HPLC diagram of $\text{CuFe}_2\text{O}_4/\text{GO}$ showed the only a single intermediate compound with very low intensity (retention time RT of 1.5 minutes). These intermediates may be carboxylic with short carbon chain [23-25]. Such catalysts $\text{CuFe}_2\text{O}_4/\text{GO}$ is highly active in the decomposition of phenol in phenolic concentration conditions first 100 mg/L, the concentration of catalyst 0.1 g/L, H_2O_2 concentration 136 mg/L, pH value of 3 using lights simulate irradiation.

d/ Stability of $\text{CuFe}_2\text{O}_4/\text{GO}$ composite

In each test, the photocatalyst was separated from the equilibrium solution by a magnet, washed with ethanol, and vacuum dried at 60°C for 6 h. As observed in fig. 9, after the first regeneration cycle, the COD removal efficiency was 90 %. After the third cycle, the COD removal efficiency of $\text{CuFe}_2\text{O}_4/\text{GO}$ was 84 %. The decrease of catalyst activity may be due to the CuFe_2O_4 leaching into the solution and/or incomplete desorption of substrates from the catalyst surface.

However, after the third reaction run, catalytic activity decreased due to its magnetic property. Moreover, it can be easily can be recovered due to its magnetic property.

4. Conclusions

- $\text{CuFe}_2\text{O}_4/\text{GO}$ composite was successfully synthesized by co-precipitation in “situ” using $\text{FeCl}_3 \cdot 6\text{H}_2\text{O}$ and $\text{CuCl}_2 \cdot 2\text{H}_2\text{O}$ as iron and copper sources on GO and followed by thermal reduction. From the XRD, XPS results, it revealed the formation of spinel CuFe_2O_4 on GO surface. From TEM images, it showed that CuFe_2O_4 composite has particle size of 20-30 nm and uniform size distribution.
- $\text{CuFe}_2\text{O}_4/\text{GO}$ composite exhibited high photo fenton activity (COD removal 90% after 90 min. reaction). The high catalytic activity of present nano CuFe_2O_4 particles can be ascribed to high catalytic surface area (due to small sized CuFe_2O_4 and GO sheets),

excellent synergistic coupling of Cu/Fe species and presence of graphene sheets which holds the organic species by π - π interactions. Additionally, this CuFe₂O₄/GO composite showed high magnetism so it can be easily recovered by applying the magnetic field out side.

ACKNOWLEDGMENTS

The authors thanks the Institute of Chemistry and Vietnam Academy of Science and Technology -VAST for financial support.

REFERENCES

- [1] Shamik Chowdhury, Rajasekhar Balasubramanian, 2014, Recent advances in the use of graphene-family nanoadsorbents for removal of toxic pollutants from wastewater, *Advances in Colloid and Interface Science*, 204, 35.
- [2] a/ Rao CN, Sood AK, Subrahmanyam KS, Govindaraj A., 2009, Graphene: the new two-dimensional nanomaterial, *Angew Chem Int Ed.*, 48, 7752-77.
b/ A. K. Geim & K. S. Novoselov, 2007, The rise of graphene, *Nature Materials*, 6, 183 – 191.
c/ Sungjin Park & Rodney S. Ruoff, 2009, Chemical methods for the production of graphenes, *Nature Nanotechnology* 4, 217 – 224.
- [3] Ravi Kant Upadhyay, Navneet Soin and Susanta Sinha Roy, 2014, Role of graphene/metal oxide composites as photocatalysts, adsorbents and disinfectants in water treatment: a review, *RSC Adv.*, 4, 3823.
- [4] Xinjuan Liu, Likun Pan, Qingfei Zhao, Tian Lv, Guang Zhu, Taiqiang Chen, Ting Lu, Zhuo Sun, Changqing Sun, 2012, UV-assisted photocatalytic synthesis of ZnO-reduced graphene oxide composites with enhanced photocatalytic activity in reduction of Cr(VI), *Chemical Engineering Journal*, 183, 238-243.
- [5] Jie Feng, Li Su, Yanhua Ma, Cuiling Ren, Qing Guo, Xingguo Chen, 2013, CuFe₂O₄ magnetic nanoparticles: A simple and efficient catalyst for the reduction of nitrophenol, *Chemical Engineering Journal*, 221(1), 16-24.
- [6] Yong Feng, Changzhong Liao, Kaimin Shih, 2016, Copper-promoted circumneutral activation of H₂O₂ by magnetic CuFe₂O₄ spinel nanoparticles: Mechanism, stoichiometric efficiency, and pathway of degrading sulfanilamide, *Chemosphere*, 154, 573-582.
- [7] Chin Kui Cheng & Zi Ying Kong & Maksudur R. Khan, 2015, Photocatalytic-Fenton Degradation of Glycerol Solution over Visible Light-Responsive CuFe₂O₄, *Water Air Soil Pollut.*, 226, 327.
- [8] Peng Chen, Xiang Xing, Huifang Xie, Qi Sheng, Hongxia Qu, 2016, High catalytic activity of magnetic CuFe₂O₄/graphene oxide composite for the degradation of organic dyes under visible light irradiation, *Chemical Physics Letters*, 660, 176-181.
- [9] Yitao Zhao, Guangyu He, Wen Dai, and Haiqun Chen, 2014, High Catalytic Activity in the Phenol Hydroxylation of Magnetically Separable CuFe₂O₄-Reduced Graphene Oxide, *Ind. Eng. Chem. Res.*, 53(32), 12566-12574.
- [10] W.S. Hummers Jr., R.E. Offerman, 1958, Preparation of graphitic oxide, *J. Am. Chem. Soc.*, 80, 1339.
- [11] Yanwu Zhu, Shanthi Murali, Meryl D. Stoller, Aruna Velamakanni, Richard D. Piner, Rodney S. Ruoff, 2010. Microwave assisted exfoliation and reduction of graphite oxide for ultracapacitors, *Carbon*, 48(7), 2118-2122.
- [12] M Kanagaraj, P Sathishkumar, G Kalai Selvan, I Phebe Kokila & S Arumugam, 2014, Structural and magnetic properties of CuFe₂O₄-prepared and thermally treated spinel nanoferrites, *Indian Journal of Pure & Applied Physics*, 52, 124-131.
- [13] X.D. Huang, X.F. Zhou, K. Qian, D.Y. Zhao, Z.P. Liu, C.Z. Yu, 2012, A magnetite nanocrystal/graphene composite as high performance anode for lithium-ion batteries, *J. Alloys Compd.*, 514, 76-80.
- [14] Li D, Muller MB, Gilje S, Kaner RB, Wallace GG, 2008, Processable aqueous dispersions of graphene nanosheets, *Nat Nanotechnol.*, 3, 101-5.
- [15] Rajasekhar Balasubramanian and Shamik Chowdhury, 2015, Recent advances and progress in the development of graphene-based adsorbents for CO₂ capture, *J. Mater. Chem. A*, 3, 21968-21989.
- [16] Bo Yang, Zhang Tian, Li Zhang, Yaopeng Guo, Shiqiang Yan, 2015, Enhanced heterogeneous Fenton degradation of Methylene Blue by nanoscale zero valent iron (nZVI) assembled on magnetic Fe₃O₄/reduced graphene oxide, *Journal of Water Process Engineering*, 5, 101-111.
- [17] Jeongho Park, Tyson Back, William C. Mitchel, Steve S. Kim, Said Elhamri, John Boeckl, Steven B. Fairchild, Rajesh Naik, and Andrey A. Voevodin, 2015, Approach to multifunctional device platform with epitaxial graphene on transition metal oxide, *Sci Rep.*, 5, 14374.
- [18] Carla Bittencourt, Adam P Hitchcock, Xiaoxing Ke, Gustaaf Van Tendeloo, Chris P Ewels, and Peter Guttman, Guttman, 2012, X-ray absorption spectroscopy by full-field X-ray microscopy of a thin graphite flake: Imaging and electronic structure via the carbon K-edge, *Beilstein J Nanotechnol.*, 3, 345-350.
- [19] Nedkov, I., Vandenbergh, R. E., Marinova, T., Thailhades, Ph., Merodiiska, T., Avramova, I., 2006, Magnetic structure and collective Jahn-Teller distortions in nanostructured particles of CuFe₂O₄, *Appl. Surf. Sci.*, 253, 2589.
- [20] Avik De, Asim K. De, Gouri Sankar Panda & Sandip Haldar, 2016, Synthesis of iron-based nanoparticles and comparison of their catalytic activity for degradation of phenolic waste water in a small-scale batch reactor, *Desalination and Water Treatment*, 57(52), 25170.
- [21] Nguyen Tri Khoa, Soon Wook Kim, Doan Van Thuan, Huynh Ngoc Tien, Seung Hyun Hur, Eui Jung Kimb and Sung Hong Hahn, 2015, Fast and effective electron transport in a Au-graphene-ZnO hybrid for enhanced photocurrent and photocatalysis, *RSC Adv.*, 5, 63964-63969.
- [22] Ritu Dhanda and Mazaahir Kidwai, 2016, Magnetically

separable CuFe₂O₄/reduced graphene oxide nanocomposites: as a highly active catalyst for solvent free oxidative coupling of amines to imines, *RSC Adv.*, 6, 53430-53437.

- [23] L.F. Liotta, M. Gruttadauria, G. Di Carlo, G. Perrini, V. Librando, 2009, Heterogeneous catalytic degradation of phenolic substrates: Catalysts activity *Journal of Hazardous Materials*, 162 (2-3), 588-606.
- [24] Yao-Hui Huang, Yu-Jen Huang, Hung-Chih Tsai, Hung-Ta Chen, 2010, Degradation of phenol using low concentration of ferric ions by the photo-Fenton process, *Journal of the Taiwan Institute of Chemical Engineers*, 41, 699-704.
- [25] A. Eftaxias, J. Font, A. Fortuny, J. Giralt, A. Fabregat, F. Stüber, 2001, Kinetic modelling of catalytic wet air oxidation of phenol by simulated annealing, *Applied Catalysis B: Environmental*, 33, 175-190.